

# Probing Strongly Correlated $4f$ -Orbital Symmetry of the Ground State in Yb Compounds by Linear Dichroism in Core-Level Photoemission

Takeo Mori,<sup>1</sup> Satoshi Kitayama,<sup>1</sup> Yuina Kanai,<sup>1</sup> Sho Naimen,<sup>1</sup> Hidenori Fujiwara,<sup>1</sup> Atsushi Higashiya,<sup>2,3</sup> Kenji Tamasaku,<sup>3,4</sup> Arata Tanaka,<sup>5</sup> Kensei Terashima,<sup>6,\*</sup> Shin Imada,<sup>6</sup> Akira Yasui,<sup>7</sup> Yuji Saitoh,<sup>8</sup> Kohei Yamagami,<sup>1</sup> Kohei Yano,<sup>1</sup> Taiki Matsumoto,<sup>1</sup> Takayuki Kiss,<sup>1,3,4</sup> Makina Yabashi,<sup>3</sup> Tetsuya Ishikawa,<sup>3</sup> Shigemasa Suga,<sup>3,9</sup> Yoshichika Ōnuki,<sup>10,†</sup> Takao Ebihara,<sup>11</sup> and Akira Sekiyama<sup>1,3,4,‡</sup>

<sup>1</sup>*Division of Materials Physics, Graduate School of Engineering Science, Osaka University, Toyonaka, Osaka 560-8531, Japan*

<sup>2</sup>*Faculty of Science and Engineering, Setsunan University, Neyagawa, Osaka 572-8508, Japan*

<sup>3</sup>*RIKEN SPring-8 Center, Sayo, Hyogo 679-5148, Japan*

<sup>4</sup>*Center for Promotion of Advanced and Interdisciplinary Research,*

*Graduate School of Engineering Science, Osaka University, Toyonaka, Osaka 560-8531, Japan*

<sup>5</sup>*Department of Quantum Matter, ADSM, Hiroshima University, Higashi-Hiroshima, Hiroshima 739-8530, Japan*

<sup>6</sup>*Department of Physical Science, Ritsumeikan University, Kusatsu, Shiga 525-8577, Japan*

<sup>7</sup>*Japan Synchrotron Radiation Research Institute, SPring-8, Sayo, Hyogo 679-5198, Japan*

<sup>8</sup>*Condensed Matter Science Division, Japan Atomic Energy Agency, SPring-8, Hyogo 679-5148, Japan*

<sup>9</sup>*Institute of Scientific and Industrial Research, Osaka University, Ibaraki, Osaka 567-0047, Japan*

<sup>10</sup>*Department of Physics, Graduate School of Science,*

*Osaka University, Toyonaka, Osaka 560-0043, Japan*

<sup>11</sup>*Department of Physics, Shizuoka University, Shizuoka 422-8529, Japan*

(Dated: April 8, 2018)

We show that the strongly correlated  $4f$ -orbital symmetry of the ground state is revealed by linear dichroism in core-level photoemission spectra as we have discovered for  $\text{YbRh}_2\text{Si}_2$  and  $\text{YbCu}_2\text{Si}_2$ . Theoretical analysis tells us that the linear dichroism reflects the anisotropic charge distributions resulting from crystalline electric field. We have successfully determined the ground-state  $4f$  symmetry for both compounds from the polarization-dependent *angle-resolved* core-level spectra at a low temperature well below the first excitation energy. The excited-state symmetry is also probed by temperature dependence of the linear dichroism where the high measuring temperatures are of the order of the crystal-field-splitting energies.

## I. INTRODUCTION

Strongly correlated electron systems show a variety of intriguing phenomena like unconventional and/or high-temperature superconductivity, spin and charge ordering, formation of heavy fermions, non-trivial (Kondo) semi-conducting behavior, and quantum criticality. Among them, such Yb-based single-crystalline compounds as  $\text{YbRh}_2\text{Si}_2$  [1] and  $\beta\text{-YbAlB}_4$  [2] showing the quantum criticality in ambient pressure, a Kondo semiconductor  $\text{YbB}_{12}$  [3, 4], valence-fluctuating  $\text{YbAl}_3$  [5, 6] and  $\text{YbCu}_2\text{Si}_2$  [7, 8], and a very heavy fermionic  $\text{YbCo}_2\text{Zn}_{20}$  [9–11] have been synthesized with excellent quality and thus intensively studied within a couple of decades. Since the strong Coulomb repulsion (effective value of 6-10 eV) works between the  $4f$  electrons in the Yb sites, an ionic picture is a good starting point to discuss and reveal their electronic structure as well as the origins of various phenomena in the crystalline solids. The majority of the Yb ions in the above-mentioned ma-

terials is in trivalent  $4f^{13}$  (one  $4f$  hole) configurations although there are to some extent  $\text{Yb}^{2+}$  ( $4f^{14}$ ) components due to the hybridization between the  $4f$  orbitals and other valence-band states crossing the Fermi level. The  $\text{Yb}^{3+}$   $4f$  levels are split by the spin-orbit coupling ( $> 1$  eV) and further split by the crystalline electric field (CEF, from a few to several tens meV) in solids as shown in Fig. 1(a).

Ground-state  $f$ -orbital symmetry determined by the CEF splitting is very fundamental information of the realistic strongly correlated electron systems. In contrast to the case of transition-metal oxides in which the electron correlations work among the  $d$ -orbital electrons, the ground-state symmetry is not straightforward revealed since it is unclear which sites act as effective “*ligands*” for the  $f$  sites. A standard experimental technique for determining the  $4f$  levels with their symmetry is to analyze the inelastic neutron scattering spectra and anisotropy in the magnetic susceptibility of single crystals. However, the magnetic  $4f$ - $4f$  excitations are often hampered by the phonon excitations with the same energy scale. Moreover, it is difficult to uniquely determine the symmetry of all  $f$  levels by the analysis of the magnetic anisotropy since there are too many free parameters for a unique description of the CEF potential. Actually, the ground-state  $4f$ -orbital symmetry is not clear for here reported  $\text{YbRh}_2\text{Si}_2$  and  $\text{YbCu}_2\text{Si}_2$  although a couple of possible

\* Present address: Research Laboratory for Surface Science, Okayama University, Okayama 700-8530, Japan

† Present address: Faculty of Science, University of the Ryukyus, Nishihara, Okinawa 903-0213, Japan

‡ sekiyama@mp.es.osaka-u.ac.jp

solutions have been proposed. Polarized neutron scattering [12] for large single crystals is principally powerful to determine the  $f$ -orbital symmetry, but time-consuming.

Recently linear dichroism (LD) in the  $3d$ -to- $4f$  soft X-ray absorption spectroscopy (XAS) [12–15] for single crystals has been reported for the heavy fermion systems with nearly  $Ce^{3+}$  ( $4f^1$ ) configurations as a powerful tool to determine the  $4f$  ground state owing to the dipole selection rules. However, it is difficult to apply this technique to probe the  $Yb^{3+}$  states since there is only single-peak structure ( $3d^9 4f^{14}$  final state) at the  $M_5$  absorption edge. On the other hand, the selection rules work also in the photoemission process while the excited electron energy is much higher than that in the absorption process. We have discovered that the atomic-like multiplet-split structure in the core-level photoemission spectra shows easily detectable LD reflecting the outer  $4f$  spatial distribution probed by the created core hole. In this letter, we demonstrate that the  $4f$ -orbital symmetry of the ground state for  $YbRh_2Si_2$  and  $YbCu_2Si_2$  in tetragonal symmetry is determined by the LD in the  $Yb 3d_{5/2}$  core-level photoemission, and further that the excited-state  $4f$  symmetry is also probed by the temperature-dependent data.  $YbRh_2Si_2$  is known as the first discovered Yb system showing quantum criticality in ambient pressure as mentioned above.  $YbCu_2Si_2$  is a counterpart of the first discovered heavy fermion superconductor  $CeCu_2Si_2$  [16] with respect to an electron-hole symmetry. However, it does not show superconductivity, being recognized as one of the valence-fluctuating systems with anisotropic magnetic susceptibility [7, 8, 17] which implies the anisotropic  $4f$ -hole spatial distribution.

## II. EXPERIMENTAL

Since the binding energy of the  $Yb 3d_{5/2}$  core-level is higher than 1.5 keV, hard X-ray photoemission spectroscopy (HAXPES) at least  $h\nu > 2.5$  keV is preferable to avoid the surface contributions deviated from the bulk ones [18, 19]. We have performed LD in HAXPES [20, 21] at BL19LXU of SPring-8 [22] by using a MBS A1-HE hemispherical photoelectron spectrometer. A Si(111) double-crystal monochromator selected 7.9 keV radiation with linear polarization along the horizontal direction (the so-called degree of linear polarization  $P_L > +0.98$ ), which was further monochromatized by a Si(620) channel-cut crystal. In order to switch the linear polarization of the excitation light from the horizontal to vertical directions, two single-crystalline (100) diamonds were used as a phase retarder with the (220) reflection placed downstream of the channel-cut crystal.  $P_L$  of the polarization-switched x-ray after the phase retarder was estimated as  $-0.96$ , corresponding to the vertically linear polarization components of 98%. Since the detection direction of photoelectrons was set in the horizontal plane with the angle to the incident photons of  $60^\circ$  as shown in Fig. 1(b), the experimental configuration at the horizon-

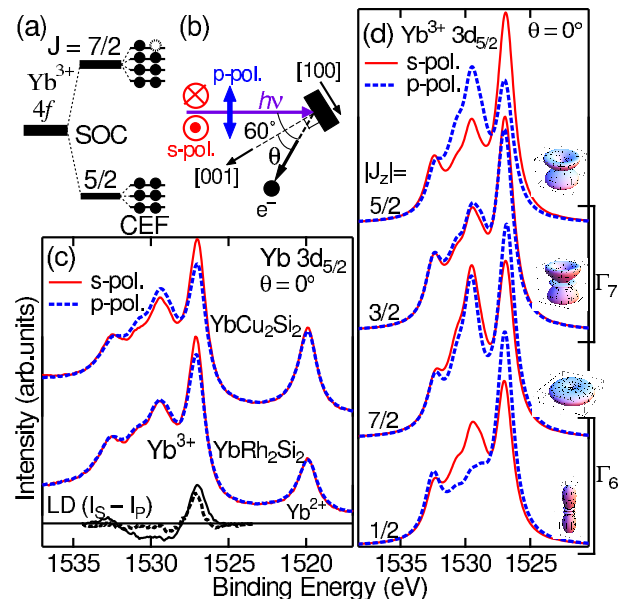


FIG. 1. (Color online) (a) Schematically drawn  $Yb^{3+} 4f$  levels split by the spin-orbit coupling (SOC) and further split by the crystalline electric field (CEF) in tetragonal symmetry. Filled (open) circle denotes an occupied  $4f$  electron (hole). (b) Geometry for the LD in HAXPES measurements, where  $\theta$  is the angle of photoelectron detection direction to the [001] direction (normal direction to the cleaved surfaces). (c) Polarization-dependent  $Yb 3d_{5/2}$  core-level HAXPES spectra for  $YbRh_2Si_2$  and  $YbCu_2Si_2$  at  $\theta = 0^\circ$  (along the [001] direction). The spectra are normalized by the overall  $3d_{5/2}$  spectral weight displayed in this graph. LD for  $YbRh_2Si_2$  ( $YbCu_2Si_2$ ) is also shown by the dashed (solid) line in the lower panel. (d) Simulated polarization-dependent  $3d_{5/2}$  photoemission spectra for the  $Yb^{3+}$  ions assuming the pure  $J_z$  ground state, together with the corresponding  $4f$ -hole spatial distributions.

tally (vertically) polarized light excitation corresponds to the p-polarization (s-polarization). The excitation light was focused onto the samples with the spot size of  $\sim 25 \mu m \times 25 \mu m$  by using an ellipsoidal Kirkpatrick-Baez mirror. The single crystals of  $YbRh_2Si_2$  and  $YbCu_2Si_2$  synthesized by a flux method were cleaved along the (001) plane *in situ*, where the base pressure was  $\sim 1 \times 10^{-7}$  Pa. The sample and surface quality was checked by the absence of any core-level spectral weight caused by a possible impurity including oxygen and carbon. The energy resolution was set to 250 meV.

## III. RESULTS AND DISCUSSIONS

The polarization-dependent  $Yb 3d_{5/2}$  core-level HAXPES spectra of  $YbRh_2Si_2$  and  $YbCu_2Si_2$  at  $\theta = 0^\circ$  (photoelectron detection is along the [001] direction) are shown in Fig.1(c). There are a single peak at the binding energy of  $\sim 1520$  eV and a multiple-peak structure rang-

ing from 1525 to 1535 eV in all spectra. Since the  $4f$  subshell is fully occupied in the  $\text{Yb}^{2+}$  sites with spherically symmetric  $4f$  distribution, the former single peak is ascribed to the  $\text{Yb}^{2+}$  states. The  $3d^9 4f^{13}$  (one  $4f$  hole with one  $3d$  core hole) final states for the  $\text{Yb}^{3+}$  components show the atomic-like multiplet-split peak structure in the 1525-1535 eV range. Clear LD defined by the difference of the spectral weight between the  $s$ - and  $p$ -polarization configurations is seen in the  $\text{Yb}^{3+} 3d_{5/2}$  spectral weight depending on material, where it is relatively weaker for  $\text{YbRh}_2\text{Si}_2$ . For instance, one of the  $\text{Yb}^{3+} 3d_{5/2}$  peak at 1527 eV is stronger in the  $s$ -polarization configuration ( $s$ -pol.) than in the  $p$ -polarization configuration ( $p$ -pol.) whereas a structure with the 1529.5-eV peak and 1530.5-eV shoulder is stronger in the  $p$ -pol. for both compounds. Possible photoelectron diffraction effects are ruled out of the origin of LD based on the fact that the degree of LD is mutually different between both compounds with the same  $\text{ThCr}_2\text{Si}_2$  crystal structure.

To clarify the origin of LD in the  $\text{Yb}^{3+} 3d_{5/2}$  core-level HAXPES spectra, we have performed ionic calculations including the full multiplet theory [23] and the local CEF splitting using the XTLS 9.0 program [24]. All atomic parameters such as the  $4f$ - $4f$  and  $3d$ - $4f$  Coulomb and exchange interactions (Slater integrals) and the  $3d$  and  $4f$  spin-orbit couplings have been obtained by Cowan's code [25] based on the Hartree-Fock method. The Slater integrals (spin-orbit couplings) are reduced down to 88% (98%) to fit the core-level photoemission spectra [26]. We show the polarization-dependent core-level spectra at  $\theta = 0^\circ$  for pure  $|J_z\rangle$  states of the  $\text{Yb}^{3+}$  ions with  $J = 7/2$  in Fig.1(d). LD depends strongly on  $|J_z|$ , reflecting the Coulomb interactions between the  $3d$  and  $4f$  holes with anisotropic spatial distributions in the final state. The result of the simulations tells us that the observed LD in the core-level HAXPES spectra originates from the anisotropic  $4f$  hole distribution under CEF in the initial state.

In the case of  $\text{Yb}^{3+}$  ions in tetragonal symmetry, the eightfold degenerate  $J = 7/2$  state splits into four doublets as

$$|\Gamma_7^1\rangle = c|\pm 5/2\rangle + \sqrt{1-c^2}|\mp 3/2\rangle, \quad (1)$$

$$|\Gamma_7^2\rangle = -\sqrt{1-c^2}|\pm 5/2\rangle + c|\mp 3/2\rangle, \quad (2)$$

$$|\Gamma_6^1\rangle = b|\pm 1/2\rangle + \sqrt{1-b^2}|\mp 7/2\rangle, \quad (3)$$

$$|\Gamma_6^2\rangle = \sqrt{1-b^2}|\pm 1/2\rangle - b|\mp 7/2\rangle, \quad (4)$$

where the coefficients  $0 \leq b \leq 1$ ,  $0 \leq c \leq 1$  defining the actual charge distributions, and CEF splitting energies depend on the CEF parameters  $B_2^0, B_4^0, B_4^4, B_6^0$ , and  $B_6^4$  in Stevens formalism [27]. Since all CEF splitting energies are highly expected to be much larger ( $\gtrsim 100$  K) than the measured temperature of 14 K for  $\text{YbRh}_2\text{Si}_2$  [28] and  $\text{YbCu}_2\text{Si}_2$  [29, 30], it is justified to assume that only the lowest state is populated. As shown in Fig.1(d), LD is qualitatively different between  $|\Gamma_6^{1,2}\rangle$  and  $|\Gamma_7^{1,2}\rangle$ , where LDs for  $|J_z| = 5/2$  and  $3/2$  are qualitatively consistent with those for the experimental data. Therefore, the

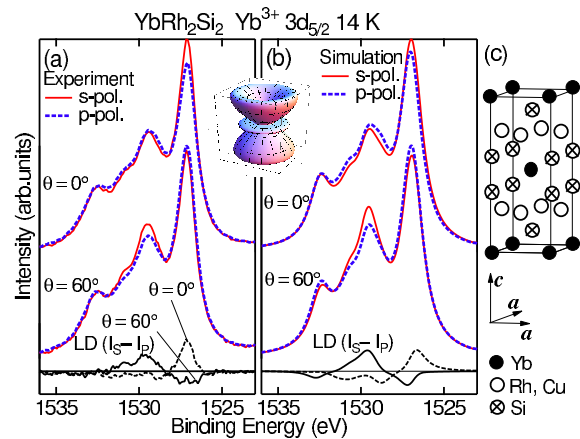


FIG. 2. (Color online) (a) Polarization-dependent  $\text{Yb}^{3+} 3d_{5/2}$  core-level HAXPES spectra of  $\text{YbRh}_2\text{Si}_2$  at  $\theta = 0^\circ$  and  $60^\circ$  and their LDs, where the Shirley-type background has been subtracted from the raw spectra. The spectra are normalized by the  $\text{Yb}^{3+} 3d_{5/2}$  spectral weight. (b) Simulated polarization-dependent core-level photoemission spectra and their LDs [dashed (solid) line for  $\theta = 0^\circ$  ( $60^\circ$ )] for the  $\text{Yb}^{3+}$  ion with the  $|J_z| = 3/2$  ( $\Gamma_7$ ) ground state at the same geometrical configurations as those for the experiments. The inset shows the corresponding  $4f$  hole spatial distribution in the initial state. (c) Crystal structure of  $\text{YbRh}_2\text{Si}_2$  and  $\text{YbCu}_2\text{Si}_2$ .

$|\Gamma_6^{1,2}\rangle$  ground state formed by the  $|J_z| = 7/2$  and  $1/2$  components is ruled out for both compounds.

To more accurately determine the ground-state orbital symmetry, we have also performed the polarization-dependent core-level HAXPES for  $\text{YbRh}_2\text{Si}_2$  at different  $\theta$  of  $60^\circ$  corresponding to the incident photon direction parallel to the  $[001]$  direction as shown in Fig.2(a). Compared to LD at  $\theta = 0^\circ$ , the sign of LD at  $\theta = 60^\circ$  is flipped as recognized at the bottom of the figure. We have found that our data are best described by the pure  $|J_z| = 3/2$  ground state as shown in Fig.2(b). So far, it has been unclear whether  $|\Gamma_6^1\rangle$  with dominant  $|J_z| = 1/2$  or  $|\Gamma_7^1\rangle$  with dominant  $|J_z| = 3/2$  forms the ground state [31, 32] while a comparison of the slab calculations for subsurface  $\text{YbRh}_2\text{Si}_2$  to the low-energy angle-resolved photoemission data has suggested the  $|\Gamma_7^1\rangle$  ground state [33]. Here the  $|J_z| = 3/2$  ( $\Gamma_7$ ) ground state is unambiguously revealed for  $\text{YbRh}_2\text{Si}_2$  from our LD in HAXPES at  $\theta = 0^\circ$  and  $60^\circ$ . Since there is no anisotropy within the  $ab$  plane for the  $4f$  hole distribution with the  $|J_z| = 3/2$  ground state as depicted in the inset of Fig. 2, it is naturally concluded that the  $\text{Yb} 4f$  holes are hybridized with the partially filled neighbor  $\text{Rh} 4d$  and  $\text{Si} 3sp$  states where the  $4f$  hole distribution spreads over both sites in Fig.2(c).

The polarization-dependent  $\text{Yb}^{3+} 3d_{5/2}$  HAXPES spectra of  $\text{YbCu}_2\text{Si}_2$  at  $\theta = 0^\circ$  and  $60^\circ$  are shown in Fig.3(a). In contrast to the data for  $\text{YbRh}_2\text{Si}_2$ , the sign of LD is not flipped between two angles of  $\theta$  whereas LD is reduced at  $\theta = 60^\circ$ , being inconsistent with the simulations for the pure  $|J_z| = 3/2$  state in Fig.2(b). Our de-

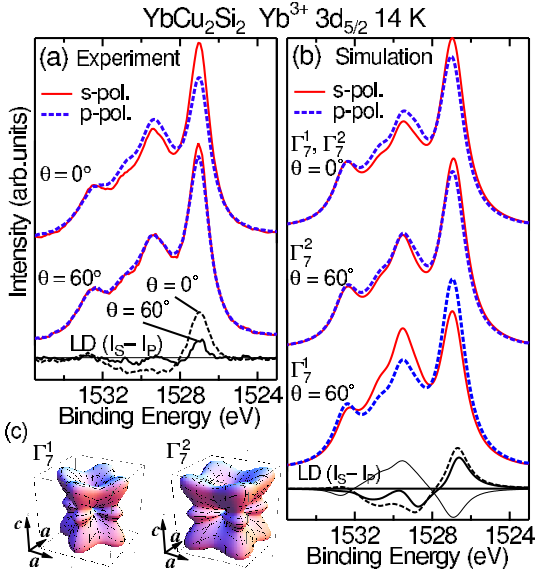


FIG. 3. (Color online) (a) Polarization-dependent  $\text{Yb}^{3+} 3d_{5/2}$  core-level HAXPES spectra of  $\text{YbCu}_2\text{Si}_2$  at  $\theta = 0^\circ$  and  $60^\circ$  and their LDs, where the Shirley-type background has been subtracted from the raw spectra. (b) Simulated polarization-dependent core-level photoemission spectra and their LDs at the same geometrical configurations as those for the experiments for the  $\text{Yb}^{3+}$  ion with the  $|\Gamma_7^1\rangle$  and  $|\Gamma_7^2\rangle$  ground states with the  $|J_z| = 3/2$  ( $5/2$ ) component of 87% (13%). LD at  $\theta = 0^\circ$  is represented by a dashed line whereas that at  $\theta = 60^\circ$  for the  $|\Gamma_7^1\rangle$  ( $|\Gamma_7^2\rangle$ ) ground state is shown by a thin (thick) solid line. (c)  $4f$  hole spatial distribution for the initial  $|\Gamma_7^1\rangle$  and  $|\Gamma_7^2\rangle$  states.

tailed analysis indicates that the data set of polarization-dependent HAXPES is best described by the ground state of

$$|\Gamma_7^2\rangle = -0.36|5/2\rangle + 0.93|3/2\rangle \quad (5)$$

as shown in Fig.3(b), where the precision of  $c^2$  in Eq.(2) is  $\pm 0.05$ . The state of  $|\Gamma_7^1\rangle = 0.36|5/2\rangle + 0.93|3/2\rangle$  with the same amount of the  $|J_z| = 3/2$  components as in Eq.(5), of which the spatial  $4f$  hole distribution shows the same shape as for  $|\Gamma_7^2\rangle$  with rotation within the  $ab$  plane by  $45^\circ$  [see Fig.3(c), hereafter called as in-plane rotation], gives the same spectra and LD as those for  $|\Gamma_7^2\rangle$  at  $\theta = 0^\circ$ . Therefore, the data at  $\theta = 60^\circ$  enable us to discriminate the in-plane rotation of the  $4f$  charge distributions and unambiguously determine the ground state. The  $4f$  hole distribution for  $|\Gamma_7^2\rangle$  is elongated along the Si sites not the Cu sites with fully occupied  $3d$  levels [8] as shown in Figs.2(c) and 3(c), leading to the conclusion that the  $4f$  holes are primarily hybridized with the Si  $3sp$  states.

The polarization-dependent  $\text{Yb}3d_{5/2}$  core-level HAXPES spectra shown here are well reproduced apart from

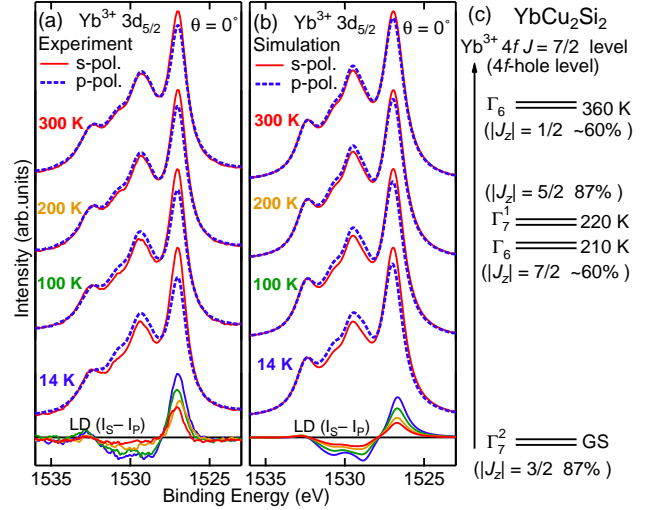


FIG. 4. (Color online) (a) Temperature dependence of the polarization-dependent  $\text{Yb}^{3+} 3d_{5/2}$  HAXPES spectra at  $\theta = 0^\circ$  and their LDs for  $\text{YbCu}_2\text{Si}_2$ . (b) Simulated temperature dependence of the polarization-dependent core-level photoemission spectra and their LDs at  $\theta = 0^\circ$  for the  $\text{Yb}^{3+}$  ion with the  $4f$  levels in (c), where the coefficient  $b^2$  in Eqs. (3) and (4) for the excited  $|\Gamma_6^{1,2}\rangle$  states of 0.4 with the lower state with predominant  $|J_z| = 7/2$  components. (c) Schematically drawn  $\text{Yb}^{3+} 4f J = 7/2$  levels with symmetry split by CEF determined for  $\text{YbCu}_2\text{Si}_2$  together with the fraction of the predominant component for each doublet.

the  $\text{Yb}^{2+}$  contributions by the simulations for the atomic-like models as seen in the analysis of many LD data in XAS for Ce compounds [12–15], where the hybridization effects are not explicitly taken into account. Such a successful analysis is owing to the highly localized nature of the  $\text{Yb}^{3+}$  sites in the  $3d$  core-level photoemission final states due to the core hole- $4f$  Coulomb interactions ( $\sim 10$  eV) giving a sufficient energy splitting between the  $\text{Yb}^{3+}$  and  $\text{Yb}^{2+}$  final states, and the configuration dependence of the hybridization strengths [34] leading to the reduced hybridization in the final states. The analysis needs to be extended by using the Anderson impurity model for strongly hybridized systems showing the core-level spectral line shape highly deviated from the atomic-like multiplet-split structure, which is not the case for the data displayed here.

We have also performed the temperature- and polarization-dependent HAXPES at  $\theta = 0^\circ$  for  $\text{YbCu}_2\text{Si}_2$  as shown in Fig.4(a), verifying that LD is reduced at high temperatures without a flip of its sign. The temperature dependence originates from a partial occupation of the excited state  $i$  split by  $\Delta_i$  from the ground state at high temperatures  $T$  with a fraction of  $\exp[-\Delta_i/(k_B T)] / \{1 + \sum_i \exp[-\Delta_i/(k_B T)]\}$ , which leads to the isotropic spec-

tra at a sufficiently high temperature. Taking the fact that the magnetic excitations are clearly seen at  $\sim 210$  and  $\sim 360$  K for  $\text{YbCu}_2\text{Si}_2$  [29] into account, we can determine to some extent the  $4f$ -orbital symmetry of the excited states based on our data and simulations, where  $|\Gamma_7^1\rangle$  with dominant  $|J_z| = 5/2$  gives larger LD than the experimental one and  $|\Gamma_6\rangle$  formed by the the  $|J_z| = 7/2$  and  $1/2$  states shows a sign-flipped LD compared to the data as suggested by the simulations in Fig. 1(d). Figure 4(b) shows one of the best simulated temperature-dependent HAXPES spectra and LDs for the  $4f$ -level scheme with symmetry shown in Fig. 4(c), which has been optimized with some ambiguities in determining the parameters. The other  $4f$ -level scheme with the first excitation energy of  $\sim 100$  K similar to a previously proposed one [30] is inconsistent with the experimental result since the simulations with this scheme give larger temperature dependence of LD involving a sign-flipping or an enhancement of LD at 100 K. Here optimized CEF splitting energies for the  $4f$ -level scheme in Fig. 4(c) is similar to another previously proposed one in Ref. 7 based on the magnetic excitations in Ref. 29.

#### IV. CONCLUSIONS

In conclusion, we have shown that the  $4f$ -orbital symmetry of the ground states as well as that of the excited states in the Yb compounds is probed by the LD in the core-level HAXPES and its  $\theta$  dependence. The ground-

state symmetry is unambiguously determined by the LD under the sole assumption that only the lowest state is populated. LD in the core-level HAXPES has the advantage over LD in XAS in discriminating the same shape of the  $4f$  charge distributions with in-plane rotation as shown for  $\text{YbCu}_2\text{Si}_2$  owing to the experimental parameter  $\theta$  in addition to the polarization. The discrimination of the in-plane rotation of charge distribution is also feasible by the polarization-dependent non-resonant inelastic X-ray scattering [35], but the throughput and energy resolution are much better for LD in the core-level HAXPES. Therefore, the experimental technique demonstrated here will be very promising to reveal the strongly correlated orbital symmetry of the ground and excited states in the atomic-like partially filled subshell in solids, complementing the neutron scattering.

#### ACKNOWLEDGMENTS

We thank T. Kadono, F. Honda, Y. Nakata, Y. Nakatani, T. Yamaguchi, H. Fuchimoto, T. Yagi, S. Tachibana, A. Yamasaki, and Y. Tanaka for supporting the experiments. This work was supported by Grant-in-Aid for Scientific Research (23654121), that for Young Scientists (23684027, 23740240, 25800205), that for Innovative Areas (20102003), the Global COE (G10) from MEXT and JSPS, Japan, and by Toray Science Foundation. The hard x-ray photoemission was performed at SPring-8 under the approval of JASRI (2014A1149).

- 
- [1] O. Trovarelli, C. Geibel, S. Mederle, C. Langhammer, F. M. Grosche, P. Gegenwart, M. Lang, S. Sparn, and F. Steglich, *Phys. Rev. Lett.* **85**, 626(2000).
  - [2] S. Nakatsuji, K. Kuga, Y. Machida, T. Tayama, T. Sakakibara, Y. Karaki, H. Ishimoto, S. Yonezawa, Y. Maeno, E. Pearson, G. G. Lonzarich, L. Balicas, H. Lee, and Z. Fisk, *Nat. Phys.* **4**, 603 (2008).
  - [3] F. Iga, N. Shimizu, and T. Takabatake, *J. Magn. Magn. Mater.* **177-181**, 337 (1998).
  - [4] T. Susaki, Y. Takeda, M. Arita, K. Mamiya, A. Fujimori, K. Shimada, H. Namatame, M. Taniguchi, N. Shimizu, F. Iga, and T. Takabatake, *Phys. Rev. Lett.* **82**, 992 (1999).
  - [5] A. L. Cornerius, J. M. Lawrence, T. Ebihara, P. S. Riseborough, C. H. Booth, M. F. Hundley, P. G. Pagliuso, J. L. Sarro, J. D. Thompson, M. H. Jung, A. H. Lacerda, and G. H. Kwei, *Phys. Rev. Lett.* **88**, 117201 (2002).
  - [6] T. Ebihara, E. D. Bauer, A. L. Cornerius, J. M. Lawrence, N. Harrison, J. D. Thompson, J. L. Sarro, M. F. Hundley, and S. Uji, *Phys. Rev. Lett.* **90**, 166404 (2002).
  - [7] N. D. Dung, Y. Ota, K. Sugiyama, T. D. Matsuda, Y. Haga, K. Kindo, M. Hagiwara, T. Takeuchi, R. Settai, and Y. Ōnuki, *J. Phys. Soc. Jpn.* **78**, 024712 (2009).
  - [8] N. D. Dung, T. D. Matsuda, Y. Haga, S. Ikeda, E. Yamamoto, T. Ishikura, T. Endo, S. Tatsuoka, Y. Aoki, H. Sato, T. Takeuchi, R. Settai, H. Harima, and Y. Ōnuki, *J. Phys. Soc. Jpn.* **78**, 084711 (2009).
  - [9] M. S. Torikachvili, S. Jia, E. D. Mun, S. T. Hannahs, R. C. Black, W. K. Neils, D. Martien, S. L. Bud'ko, and P. C. Canfield, *Proc. Natl. Acad. Sci. U.S.A.* **104**, 9960 (2007).
  - [10] Y. Saiga, K. Matsubayashi, T. Fujiwara, M. Kosaka, S. Katano, M. Hedo, T. Matsumoto, and Y. Uwatoko, *J. Phys. Soc. Jpn.* **77**, 053710 (2008).
  - [11] M. Ohta, M. Matsushita, S. Yoshiuchi, T. Takeuchi, F. Honda, R. Settai, T. Tanaka, Y. Kubo, and Y. Ōnuki, *J. Phys. Soc. Jpn.* **79**, 083601 (2010).
  - [12] T. Willers, B. Fåk, N. Hollmann, P. O. Körner, Z. Hu, A. Tanaka, D. Schmitz, M. Enderle, G. Lapertot, L. H. Tjeng, and A. Severing, *Phys. Rev. B* **80**, 115106 (2009).
  - [13] P. Hansmann, A. Severing, Z. Hu, M. W. Haverkort, C. F. Chang, S. Klein, A. Tanaka, H. H. Hsieh, H.-J. Lin, C. T. Chen, B. Fåk, P. Lejay, and L. H. Tjeng, *Phys. Rev. Lett.* **100**, 066405 (2008).
  - [14] T. Willers, Z. Hu, N. Hollmann, P. O. Körner, J. Gergner, T. Burnus, H. Fujiwara, A. Tanaka, D. Schmitz, H. H. Hsieh, H.-J. Lin, C. T. Chen, E. D. Bauer, J. L. Sarro, E. Goremychkin, M. Koza, L. H. Tjeng, and A. Severing, *Phys. Rev. B* **81**, 195114 (2010).
  - [15] T. Willers, D. T. Adroja, B. D. Rainford, Z. Hu, N. Hollmann, P. O. Körner, Y.-Y. Chin, D. Schmitz, H. H. Hsieh, H.-J. Lin, C. T. Chen, E. D. Bauer, J. L. Sarro, K. J. McClellan, D. Byler, C. Geibel, F. Steglich, H. Aoki,

- P. Lejay, A. Tanaka, L. H. Tjeng, and A. Severing, Phys. Rev. B **85**, 035117 (2012).
- [16] F. Steglich, J. Aarts, C. D. Bredl, W. Lieke, D. Meschede, W. Franz, and H. Schäfer, Phys. Rev. Lett. **43**, 1892 (1979).
- [17] L. Moreschini, C. Dallera, J. J. Joyce, J. L. Sarrao, E. D. Bauer, V. Fritsch, S. Bobev, E. Carpene, S. Huotari, G. Vankó, G. Monaco, P. Lacovig, G. Panaccione, A. Fondacaro, G. Paolicelli, P. Torelli, M. Grioni, Phys. Rev. B **75**, 035113 (2007).
- [18] S. Suga, A. Sekiyama, S. Imada, A. Shigemoto, A. Yamasaki, M. Tsunekawa, C. Dallera, L. Braicovich, T.-L. Lee, O. Sakai, T. Ebihara, and Y. Ōnuki, J. Phys. Soc. Jpn. **74**, 2880 (2005).
- [19] S. Kitayama, H. Fujiwara, A. Gloskovski, M. Gorgoi, F. Schaefers, C. Felser, G. Funabashi, J. Yamaguchi, M. Kimura, G. Kuwahara, S. Imada, A. Higashiya, K. Tamasaku, M. Yabashi, T. Ishikawa, Y. Ōnuki, T. Ebihara, S. Suga and A. Sekiyama, J. Phys. Soc. Jpn. **81**, SB055 (2012).
- [20] A. Sekiyama, J. Yamaguchi, A. Higashiya, M. Obara, H. Sugiyama, M. Y. Kimura, S. Suga, S. Imada, I. A. Nekrasov, M. Yabashi, K. Tamasaku, and T. Ishikawa, New J. Phys. **12**, 043045 (2010).
- [21] A. Sekiyama, A. Higashiya, and S. Imada, J. Electron Spectrosc. Relat. Phenom. **190**, 201 (2013).
- [22] M. Yabashi, K. Tamasaku, and T. Ishikawa, Phys. Rev. Lett. **87**, 140801 (2001).
- [23] B. T. Thole, G. van der Laan, J. C. Fuggle, G. A. Sawatzky, R. C. Karnatak and J.-M. Esteve, Phys. Rev. B **32**, 5107 (1985).
- [24] A. Tanaka and T. Jo, J. Phys. Soc. Jpn. **63**, 2788 (1994).
- [25] R. D. Cowan, *The Theory of Atomic Structure and Spectra* (University of California Press, Berkeley, 1981).
- [26] J. Yamaguchi, A. Sekiyama, S. Imada, H. Fujiwara, M. Yano, T. Miyamachi, G. Funabashi, M. Obara, A. Higashiya, K. Tamasaku, M. Yabashi, T. Ishikawa, F. Iga, T. Takabatake, and S. Suga, Phys. Rev. B **79**, 125121 (2009).
- [27] K.W. H. Stevens, Proc. Phys. Soc. London Sect. A **65**, 209 (1952).
- [28] O. Stockert, M. M. Koza, J. Ferstl, A. P. Murani, C. Geibel, and F. Steglich, Physica B **378-380**, 157 (2006).
- [29] E. Holland-Moritz, D. Wohlleben, and M. Loewenhaupt, Phys. Rev. B **25**, 7482 (1982).
- [30] A. Yu. Muzychka, JETP **87**, 162 (1998).
- [31] A. M. Leushin and V. A. Ivanshin, Physica B **403**, 1265 (2008).
- [32] A. S. Kutuzov, A. M. Skvortsova, S. I. Belov, J. Sichelschmidt, J. Wykhoff, I. Ermin, C. Krellner, C. Geibel, and B. I. Kochelaev, J. Phys.: Condens. Matter **20**, 455208 (2008).
- [33] D. V. Vyalikh, S. Danzenbächer, Yu. Kucherenko, K. Kummer, C. Krellner, C. Geibel, M. G. Holder, T. K. Kim, C. Laubschat, M. Shi, L. Patthey, R. Follath, and S. L. Molodtsov, Phys. Rev. Lett. **105**, 237601 (2010).
- [34] O. Gunnarsson and O. Jepsen, Phys. Rev. B **38**, 3568 (1988).
- [35] T. Willers, F. Strigari, N. Hiraoka, Y. Q. Cai, M. W. Haverkort, K.-D. Tsuei, Y. F. Liao, S. Seiro, C. Geibel, F. Steglich, L. H. Tjeng, and A. Severing, Phys. Rev. Lett. **109**, 046401 (2012).